energies

MDPI

Article

Computationally Efficient State-of-Charge Estimation in Li-Ion Batteries Using Enhanced Dual-Kalman Filter †

Ali Wadi [1], Mamoun Abdel-Hafez [1] and Ala A. Hussein [2,3,*]

[1] Department of Mechanical Engineering, American University of Sharjah, Sharjah P.O. Box 26666, United Arab Emirates; awadi@aus.edu (A.W.); mabdelhafez@aus.edu (M.A.-H.)
[2] Department of Electrical Engineering, Prince Mohammad Bin Fahd University, Khobar 31952, Saudi Arabia
[3] Florida Solar Energy Center, University of Central Florida, Orlando, FL 32922-5703, USA
* Correspondence: ahussein@ieee.org
† This paper is an extended version of our paper published in the 2021 4th International Symposium on Advanced Electrical and Communication Technologies (ISAECT), Alkhobar, Saudi Arabiaheld, 6–8 December 2021.

Abstract: This paper proposes a state-of-charge estimation technique to meet highly dynamic power requirements in electric vehicles. When the power going in/out the battery is highly dynamic, the statistics of the measurement noise are expected to deviate and maybe change over time from the expected laboratory specified values. Therefore, we propose to integrate adaptive noise identification with the dual-Kalman filter to obtain a robust and computationally-efficient estimation. The proposed technique is verified at the pack and cell levels using a 3.6 V lithium-ion battery cell and a 12.8 V lithium-ion battery pack. Standardized electric vehicle tests are conducted and used to validate the proposed technique, such as dynamic stress test, urban dynamometer driving schedule, and constant-current discharge tests at different temperatures. Results demonstrate a sustained improvement in the estimation accuracy and a high robustness due to immunity to changes in the statistics of the process and measurement noise sequences using the proposed technique.

Keywords: Li-ion battery; electric vehicle (EV); extended Kalman filter (EKF); cubature Kalman filter (CKF); state of charge (SOC)

Citation: Wadi, A.; Abdel-Hafez, M.; Hussein, A.A. Computationally Efficient State-of-Charge Estimation in Li-Ion Batteries Using Enhanced Dual-Kalman Filter. *Energies* **2022**, *15*, 3717. https://doi.org/10.3390/en15103717

Academic Editors: Daniel J. Auger and Jorge Barreras

Received: 31 March 2022
Accepted: 17 May 2022
Published: 19 May 2022

1. Introduction

The state of charge (SOC) is an extremely important parameter that must be tracked accurately in real time to maximize the performance of electric vehicles (EVs). Almost all available EV SOC estimation methods found in literature fall under the following three categories: (1) current-integration methods, (2) model-based methods, including variants of Kalman-filter algorithms, and (3) non-model-based methods, such as neural networks. Due to the nature of the current-integration method, which tracks the SOC in an open-loop manner by integrating the current going in/out the battery over time, inaccurate results are produced with repeated cycles. This is a result of the error accumulation in the current measurement, and hence it is considered inadequate for EV applications.

With the circular dependence of the battery's internal parameters and SOC, improving the estimation accuracy of one will lead to improvement in the other. Most equivalent-circuit models found in the literature represent the internal parameters mainly by a resistance connected in series with an RC filter [1–4], as shown in Figure 1b. In this figure, the series resistance, R_k, represents the ohmic losses (I^2R) in the form of heat, while the RC filter accounts for the time constant that emulates the transient behavior of the cell when exposed to charge/discharge pulses. Since the internal parameters vary with temperature, load current, and SOH [5–7], these parameters, in general, and most importantly the internal resistance, must be dynamically estimated to ensure accurate SOC estimation. Other battery cell modeling techniques include physics-informed models that are based on an electrochemical analysis of a battery cell [8,9]. While these models help explain the

underlying electrochemistry within the battery cell and understand the dependence of the battery cell model parameters on factors such as discharge rate and temperature changes, they are often more complex than the equivalent-circuit-based models with many more parameters that need to be identified. Further, these models are reportedly more suited for battery cell life prediction as well as characterization of battery cell decay [10]. In this paper, we opt to use an equivalent-circuit model for its relatively simple mathematical form which makes it attractive to run on embedded hardware that a battery management system would run on.

In [11], an adaptive extended Kalman filter (EKF) method is proposed for battery SOC estimation in EVs. This method has an improved performance compared to the traditional EKF since it reduces the filter dependence on the battery model by accounting for model inaccuracy and system noise. More EKF-based techniques are proposed in [12–18] for battery SOC estimation. The main limitation of the majority of existing KF-based SOC estimation methods, besides their several advantages, is that they assume a white measurement noise with zero mean and known covariance, which is not necessarily true in EVs. These methods may give inaccurate estimates and may have convergence issues if a sudden change in the internal resistance or the measurement noise statistics occur.

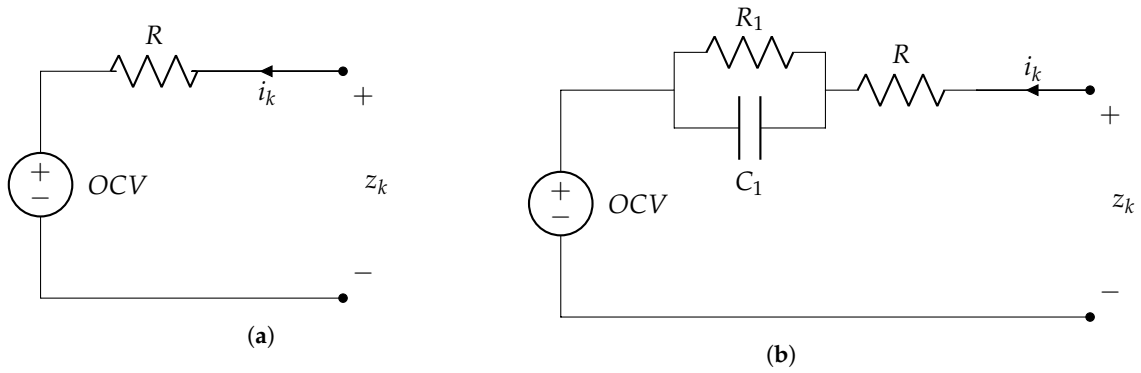

Figure 1. Equivalent circuit models used to describe battery cell dynamics. (**a**) Common Simple Model. (**b**) RC Model.

In [19,20], an unscented Kalman filter (UKF) and an adaptive EKF algorithm are proposed for estimating the battery internal resistance and SOC concurrently in real time. In general, UKFs outperform EKFs as the former has a higher capability in dealing with nonlinear systems [21]. However, the methods in [19,20] use a battery model with many parameters that are uneasy to find practically and that assume a pre-existing knowledge of the measurement noise covariance, which is not necessarily true from a practical perspective.

In [22], two methods were proposed to optimize the performance of the EKF for high-accuracy SOC estimation. The first is based on multiple model EKF and the second is based on the use of the autocovariance least squares (ALS) technique. It was shown that while both methods enhance the accuracy of SOC estimation, the ALS technique produces high-integrity and high-accuracy SOC estimation. In the referenced work, two assumptions were made on the internal resistance: first, it is known, and second, it is constant. These assumptions are impractical assumptions for an EV application where the internal parameters of the battery vary with operating conditions.

In [23], a different approach was used for modeling the internal parameters. In that method, a neural network was trained and used to track the internal parameters of the battery at a given input set, and a modified UKF was then used to estimate the SOC. Although that method resulted in an improved accuracy compared to other existing KF methods, it has a high implementation cost and requires a huge bank of data to model the neural network. Another modified EKF method is proposed in [24]. In the referenced method, a maximum likelihood estimation EKF (MLE-EKF) algorithm is proposed that addresses the uncertainties in both the process and measurement noises. However, that

method is based on a static cell model. If the parameters of the model change due to change in temperature, aging, etc., the accuracy of the method will fall.

Besides model-based SOC estimation algorithms, which consist mainly of EKF/UKF based methods, artificial neural networks (ANNs) have been also proposed for SOC estimation [25,26]. In the referenced methods, an NARX ANN technique is proposed for SOC estimation. This technique was tested using different Li-ion battery cells under constant-current pulses. In these methods, the difference between the actual and predicted SOC was fed back to the input of the network to adjust the weight functions. Practically, the actual SOC cannot be measured, and hence, the assumption that the actual SOC is provided during testing is not practical. In addition, it is unclear how these methods will behave if a battery pack that consists of series-parallel cell combinations is tested, or if a harsh test such as the DST that consists of a number of aggressive charge/discharge pulses over the full SOC range is conducted. Other ANN-based methods have been proposed in [27–31] for estimating the SOC. These methods have focused mainly on improving the speed of convergence of the ANN algorithm by replacing the standard backpropagation algorithm by other algorithms, such as the lighting search algorithm [27], backtracking algorithm [28], particle swarm optimization algorithm [29,30], and gravitational search algorithm [31]. These methods, however, were validated using a single battery cell only. Moreover, it is unclear in these works whether the true or the estimate of the SOC was used in the feedback loop during testing. In [32], a deep neural network is proposed for SOC estimation. Although deep neural networks in general are more accurate than conventional neural networks, deep neural networks have an increased complexity due to the large number of layers they use between the input and the output layers, which, as a result, increases the implementation cost, and moreover, could reduce the convergence speed.

This paper proposes a new method for enhancing the SOC estimation accuracy. The method employs a modified version of the dual KF, called DKF, that estimates the parameters and the SOC. This paper is an extended version of [33] previously submitted to the 2021 International Symposium on Advanced Electrical and Communication Technologies. The proposed method has several advantages, such as (1) it overcomes the limitations of traditional KF-based algorithms by accounting for the unknown noise covariance magnitudes in real time, which is more practical for an EV application, and (2) it is very accurate; compared to [23], a 94% MAE reduction was achieved using the proposed method through a standardized DST procedure, while a 51% MAE reduction was achieved compared to the recently proposed method in [24] through a standardized UDDS cycle. A significant number of DKF approaches in the literature are aimed at estimating the capacity of the battery cell [34,35]. Compared to works estimating the parameters of the battery [36,37], the proposed approach identifies and compensates for varying dynamics and measurements noise covariance magnitudes, and it utilizes very simple dynamics and measurements models to realize highly accurate SOC tracking with errors consistently below 1%. The simple model is advantageous when it comes to significantly reducing the computational complexity required to run the algorithm, and it could also prove beneficial to the observability of the parameters of the battery. Concerns about observability arise as the parameters to be identified are derived from a single voltage measurement at each time epoch [37,38].

The organization of this paper is as follows: in Section 2, the proposed method is derived. In Section 3, experimental results followed by discussion are presented. Finally, summary and conclusions are given in Section 4.

2. Proposed Enhanced Dual-KF Approach

All KF-based methods require the knowledge of a dynamic battery model. Referring to the models shown in Figure 1, we aim to utilize the simpler model in Figure 1a in an adaptive framework that can compensate for model shortcomings, be immune to model parameter variation, and have low computational implementation cost. The voltage of this model is given by

$$z_k = OCV(x_k) + i_k R_k \quad (1)$$

where z_k is the model voltage, i_k is the cell terminal current (assumed positive during charging and negative during discharging), OCV is the open-circuit voltage of the cell, x_k is the SOC, and R_k is the internal charge or discharge resistance.

The state of charge can be modeled as

$$x(t) = x(0) + \eta \int_0^t \frac{i(\tau)}{C_n} d\tau + \tilde{w} \tag{2}$$

where η is the (dis)charging efficiency and is assumed to be 100% for a Li-ion battery, C_n is the nominal capacity of the battery in ampere-seconds ($A.s$), and $\tilde{w}$ is the continuous-time white process noise. The discretized form of (2) is given by

$$\begin{aligned} x_{k+1} =& f(x_k, i_k) + w_k \\ =& x_k + \frac{\eta \Delta t}{C_n} i_k + w_k \end{aligned} \tag{3}$$

where $w_k \sim \mathcal{N}(0, Q_w)$ and Q_w is the process noise covariance matrix. Using Equation (1), the output voltage as a function of the SOC perturbed by white noise is given by

$$\begin{aligned} z_k =& h(x_k, i_k, \theta_k) + v_k \\ =& OCV(x_k) + i_k R_k + v_k \end{aligned} \tag{4}$$

where $v_k \sim \mathcal{N}(0, R_v)$ and R_v is the process noise covariance matrix.

In order to estimate the SOC and the model parameters, two variants of the Kalman filter will be used, namely the dual extended Kalman filter (DEKF) and the dual cubature Kalman filter (DCKF), which is an extension of the joint KF. In the joint EKF algorithm, the parameters vector θ to be estimated is augmented to the state vector. Let χ represent the stacked vector given by

$$\chi_k = \begin{bmatrix} x_k \\ \theta_k \end{bmatrix} \tag{5}$$

where x_k is the SOC and θ_k is the parameter. Furthermore, the dynamic equation of θ is given by

$$\theta_{k+1} = \theta_k + r_k \tag{6}$$

where $r_k \sim \mathcal{N}(0, Q_r)$ and Q_r is the process noise covariance matrix associated with the resistance R. The overall process covariance matrix Q is given by

$$Q = \begin{bmatrix} Q_w & 0 \\ 0 & Q_r \end{bmatrix} \tag{7}$$

The measurement covariance matrix R_v is not changed since the same measurement is used for state and parameter estimation. Algorithm 1 shows the joint extended Kalman filter (EKF) algorithm [39]. Instead of having the state and parameters stacked in a vector, as in the case of the joint EKF, the DKF algorithm uses separate Kalman filters for state and parameter estimation. This reduces the dimensionality of the state vector and hence results in simpler matrix operations and a reduction in the overall computational complexity. Therefore, the DKF algorithm will be used for practical estimation of the battery's internal resistance and SOC. The dynamic and measurement equations for parameter estimation are as follows:

$$\begin{aligned} \theta_{k+1} =& \theta_k + r_k \\ z_k =& OCV(x_k) + i_k R_k + e_k \end{aligned} \tag{8}$$

where $e_k \sim \mathcal{N}(0, R_e)$ and R_e is the estimation error covariance matrix. The state and parameter filters are first initialized as

$$\begin{aligned} \hat{x}_k \leftarrow x_0, \hat{P}_k^x \leftarrow P_{x_0} \\ \hat{\theta}_k \leftarrow \theta_0, \hat{P}_k^\theta \leftarrow P_{\theta_0} \end{aligned} \tag{9}$$

In general, $\bar{x}_k$ refers to the *a priori* estimate of x_k given measurements up to time $k-1$, whereas $\hat{x}_k$ refers to the *a posteriori* estimate of x_k given measurements up to time k. This notation similarly applies to θ_k and P_k. The state filter is then propagated through time as follows:

$$\begin{aligned} \bar{P}_{x,k+1} &= \hat{P}_{x,k} + Q_{w,k} \\ \bar{x}_{k+1} &= \hat{x}_k + \frac{\eta \Delta t}{C_n} i_k \\ H_k^x &= \frac{\delta h(x_k, i_k, \bar{\theta}_k)}{\delta x} \mid_{x=\bar{x}_k} = \frac{z_k(\bar{x}_k) - z_{k-1}(\bar{x}_{k-1})}{\bar{x}_k - \bar{x}_{k-1}} \\ K_k^x &= P_{x,k}(H_k^x)^T [H_k^x \bar{P}_{x,k}(H_k^x)^T + R_{v,k}]^{-1} \end{aligned} \tag{10}$$

Similarly, the parameter filter is propagated through time using

$$\begin{aligned} \bar{P}_{\theta,k+1} &= \hat{P}_{\theta,k} + Q_{r,k} \\ \bar{\theta}_{k+1} &= \hat{\theta}_k \\ H_k^x &= \frac{\delta h(\bar{x}_k, i_k, \theta_k)}{\delta \theta} \mid_{\theta=\bar{\theta}_k} = i_k \\ K_k^\theta &= P_{\theta,k}(H_k^\theta)^T [H_k^\theta \bar{P}_{\theta,k}(H_k^\theta)^T + R_{e,k}]^{-1} \end{aligned} \tag{11}$$

Finally, the state and parameter filters are updated as follows:

$$\begin{aligned} \bar{z}_k^x &= h(\bar{x}_k, i_k, \bar{\theta}_k) \\ \hat{x}_k &= \bar{x}_k + K_k^x (z_k - \bar{z}_k^x) \\ \hat{P}_{x,k} &= (I - K_k^x H_k^x) \bar{P}_{x,k} \\ \bar{z}_k^\theta &= h(\bar{x}_k, i_k, \bar{\theta}_k) \\ \hat{\theta}_k &= \bar{\theta}_k + K_k^\theta (z_k - \bar{z}_k^\theta) \\ \hat{P}_{\theta,k} &= (I - K_k^\theta H_k^\theta) \bar{P}_{\theta,k} \end{aligned} \tag{12}$$

Algorithm 1: The joint extended Kalman filter.

begin Initialize the filter
  $\hat{\chi}_k \leftarrow \chi_0, \hat{P}_k^\chi \leftarrow P_{\chi_0}$
  for $k = 1 \rightarrow end$ **do**
    Time Propogation:
    $\bar{P}_{\chi,k+1} = \hat{P}_{\chi,k} + Q_{w,k}$
    $\bar{\chi}_{k+1} = \hat{\chi}_k + F(\chi_k, i_k)$
    $H_k^\chi = \frac{\delta h(\bar{\chi}_k, i_k)}{\delta \chi} \mid_{\chi=\bar{\chi}_k}$
    Time Update:
    $\hat{\chi}_k = \bar{\chi}_k + K_k^\chi (z_k - h(\bar{\chi}_k, i_k))$
    $\hat{P}_{\chi,k} = (I - K_k^\chi H_k^\chi) \bar{P}_{\chi,k}$
  end
end

$$F(\chi_k, i_k) = \begin{bmatrix} f(x_k, i_k) \\ \theta_k \end{bmatrix}$$

where:

$$H_k^\chi = \frac{\delta h(\bar{\chi}_k, i_k)}{\delta \chi} \mid_{\chi=\bar{\chi}_k} = \begin{bmatrix} \frac{z_k(\bar{x}_k) - z_{k-1}(\bar{x}_{k-1})}{\bar{x}_k - \bar{x}_{k-1}} \\ i_k \end{bmatrix}$$

The aforementioned approach is to also be tested using the cubature Kalman filter (CKF). For brevity, the CKF algorithm is shown in Algorithm 2.

Algorithm 2: The cubature Kalman filter.

begin Initialize the filter

$\hat{x}_k \leftarrow x_0, \hat{P}_k \leftarrow P_{x_0}$

for $k = 1 \rightarrow end$ **do**

Time Propogation:

$$S_k = \sqrt{\hat{P}_k}$$
$$x_k^{(i)} = S_k \xi^{(i)} + \hat{x}_k, \; i = 1, 2, \ldots 2n$$
$$\chi_k^{(i)} = f(x_k^{(i)}, u_k)$$
$$\bar{x}_{k+1} = \frac{1}{2n} \sum_{i=1}^{2n} \chi_k^{(i)}$$
$$\bar{P}_{k+1} = \frac{1}{2n} \sum_{i=1}^{2n} (\chi_k^{(i)} - \bar{x}_{k+1})(\chi_k^{(i)} - \bar{x}_{k+1})^T + Q_w$$

Time Update:

$$S_{k+1} = \sqrt{\bar{P}_{k+1}}$$
$$\bar{x}_{k+1}^{(i)} = S_{k+1} \xi^{(i)} + \bar{x}_{k+1}, \; i = 1, 2, \ldots 2n$$
$$y_{k+1}^{(i)} = h(\bar{x}_{k+1}^{(i)}, u_k)$$
$$\bar{y}_{k+1} = \frac{1}{2n} \sum_{i=1}^{2n} y_{k+1}^{(i)}$$
$$P_{k+1}^{y} = \frac{1}{2n} \sum_{i=1}^{2n} (y_{k+1}^{(i)} - \bar{y}_{k+1})(y_{k+1}^{(i)} - \bar{y}_{k+1})^T + R_v$$
$$P_{k+1}^{xy} = \frac{1}{2n} \sum_{i=1}^{2n} (x_{k+1}^{(i)} - \bar{x}_{k+1})(y_{k+1}^{(i)} - \bar{y}_{k+1})^T$$
$$K_{k+1} = P_{k+1}^{xy} (P_{k+1}^{y})^{-1}$$
$$\hat{x}_{k+1} = \bar{x}_{k+1} + K_{k+1}(z_{k+1} - \bar{y}_{k+1})$$
$$\hat{P}_{k+1} = \bar{P}_{k+1} - K_{k+1} P_{k+1}^{y} K_{k+1}^T$$

end

end

where:

$$\xi^{(i)} = \begin{cases} +\sqrt{n}[1]_{(i)} & i = 1, 2, \ldots n \\ -\sqrt{n}[1]_{(i)} & i = n+1, n+2, \ldots 2n \end{cases}$$

$[1]_{(i)}$ is the i^{th} column of the $I \in R^{n \times n}$ identity matrix.

$\chi_k^{(i)}$ are the cubature points.

$\sqrt{X}$ is the matrix square root of X.

The DKF assumes the knowledge of the measurement noise statistics, which could result in a degradation in the estimator's performance if the statistics are not sufficiently accurate. Therefore, covariance matching to adapt the noise covariance magnitudes is employed to account for the unknown dynamics and measurements covariances. Even if the noise covariance magnitudes are known a priori, they may change due to aging of the system and/or its sensors [40].

The approaches proposed in [41,42] are implemented to adapt the EKF and the CKF. This procedure is suitable for real-time online applications, and the noise statistics used in the filters are left to adapt continuously during testing. If the accuracy of the system model changes with time due to environmental conditions or aging of the battery, that could also be compensated for by an increase in the measurement noise covariance. A demonstration of this method is shown in Figure 2.

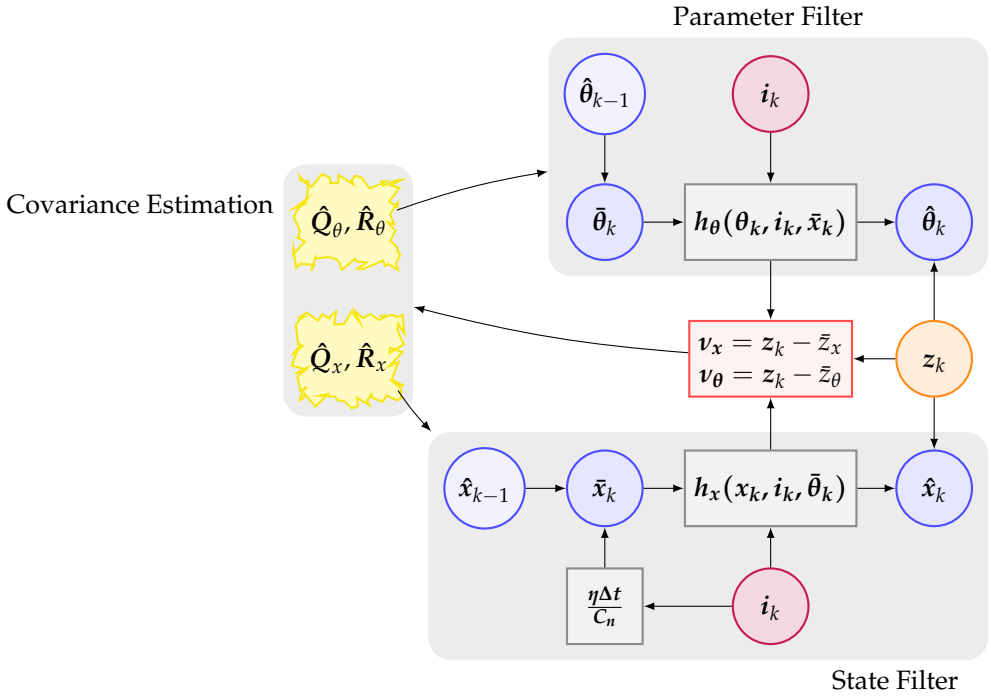

Figure 2. Block diagram of the proposed enhanced dual-Kalman-filter.

The adaptation of the EKF filter noise covariance magnitudes is summarized by the following set of equations:

$$\begin{aligned} \hat{Q}_{k+1} &= K_{k+1}\nu_{k+1}\nu_{k+1}^T K_{k+1}^T \\ \hat{R}_{k+1} &= \nu_{k+1}\nu_{k+1}^T - H_{k+1}\bar{P}_{k+1}H_{k+1}^T \end{aligned} \tag{13}$$

where ν represents the innovation sequence in Figure 2, and the other quantities are as defined in the EKF equations.

In order to have more stable estimates, a forgetting factor-based approach can be implemented to weigh the previous noise covariance magnitude estimates as shown below.

$$\begin{aligned} \hat{Q}_{k+1} &= \alpha\hat{Q}_{k+1} + (1-\alpha)\hat{Q}_k \\ \hat{R}_{k+1} &= \alpha\hat{R}_{k+1} + (1-\alpha)\hat{R}_k \end{aligned} \tag{14}$$

where the forgetting factor $0 < \alpha < 1$ can be used to filter sudden spikes in the estimates and place more weight on more recent measurements. α can be set empirically, or it can be defined as the momentum constant $\alpha = \frac{1-\beta}{1-\beta^k}$ with $0 < \beta < 1$ set as desired.

Similarly, as detailed in [42], the CKF noise covariance magnitude adaptation equations can be formulated.

3. Experimental Verification and Discussion

The proposed method is evaluated experimentally through different tests, as detailed in this section. In the described tests, the actual values of the SOC are computed using coulomb counting and indicated as "truth", while the estimated SOC is indicated by the filter used to generate the estimate. The coulomb counting technique is only used to obtain the ground truth on the assumption of known initial condition. In the presented tests, this initial state, as well as the dynamic model noise, are unknown, and the KF-based approach compensates for the coulomb counting shortcomings through the measurement update.

3.1. Test 1: Pulse Tests

In this section, a few tests are run on a 3.6 V cell that are less dynamic and not as extreme in nature than the DST or the UDDS tests presented in the next sections; namely, charging/discharging constant and variable pulse tests. The results for these are in Figure 3a,b . The performance of the proposed approach is consistently excellent, as shown in Table 1, where the MAE between the approaches is presented.

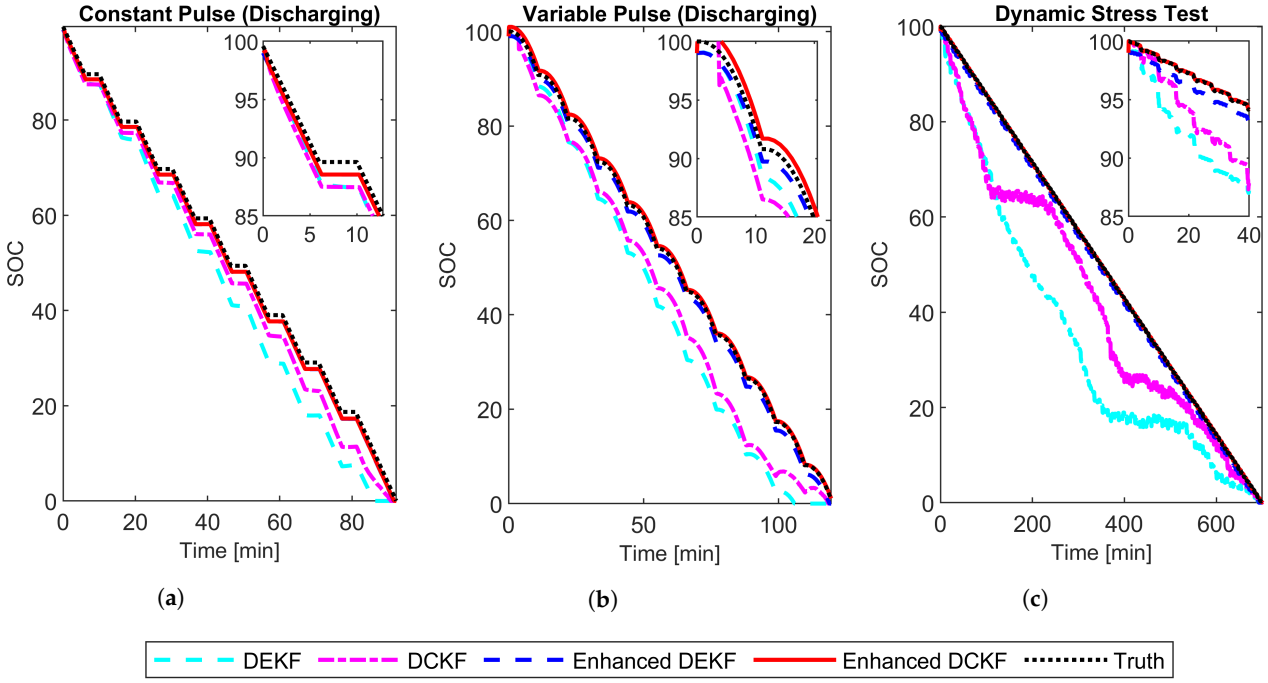

Figure 3. Performance evaluation of the dual Kalman filter variants in different battery cycles. (**a**) Constant discharge test. (**b**) VPT discharge test. (**c**) DST test.

Table 1. Mean absolute estimation error.

	Traditional		**Proposed**	
	DEKF	**DCKF**	**EDEKF**	**EDCKF**
Constant Pulse (Discharging)	6.81	3.67	1.00	0.97
Variable Pulse (Discharging)	9.81	7.70	1.32	0.65
Dynamic Stress Test	15.90	7.55	0.99	0.04
UDDS	18.61	5.32	0.15	0.05

It is necessary to comment on the discrepancy between using EKF and CKF in the proposed approach. As evident in all the testing, the DEKF generally lags behind, and we reason that to be due to the codependency between SOC estimation and parameter estimation. Unlike the EDEKF, the EDCKF is quick enough and effective at producing accurate estimates. That is, the model parameters are quickly identified and the SOC is consequently correctly identified. In terms of MAE, the proposed approach with the EDCKF achieves 0.81% on average in the two pulse tests.

3.2. Test 2: Pack DST Test

This test comprises extremely aggressive 115 DST cycles performed using a 12.8 V Li-ion battery pack covering the entire SOC range from 100% down to 0%. The purpose of this test is to evaluate the proposed techniques when exposed to highly dynamic and stressful charge or discharge power pulses using a battery pack that consists of series/parallel connected cells. The first five cycles of this test are demonstrated in Figure 4c.

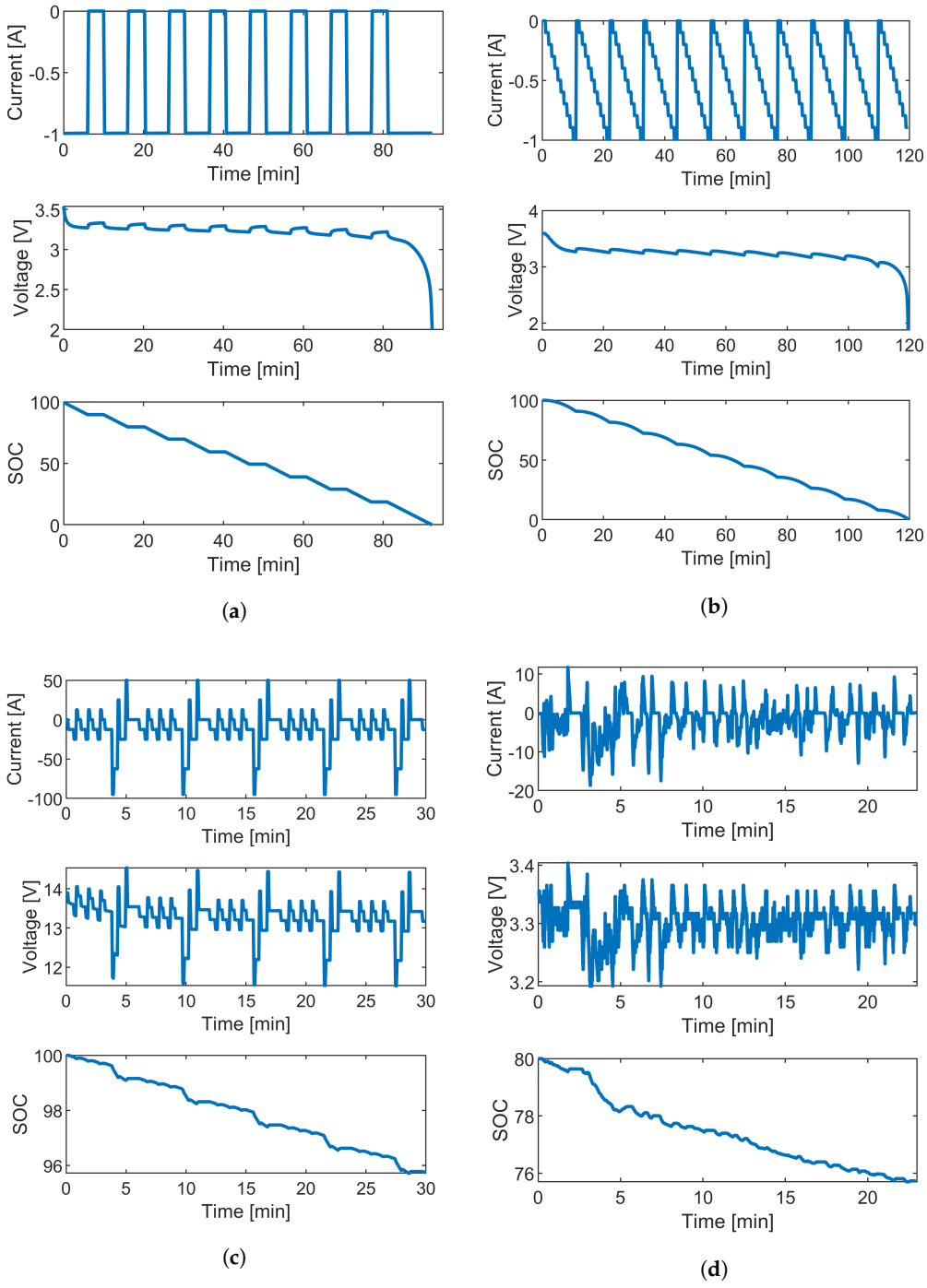

Figure 4. Test profiles showing current, voltage, and SOC sequences for the battery cell from a fully charged state to fully drained (**a**) Constant Pulse Discharge Test. (**b**) Variable Pulse Discharge Test. (**c**) DST test (cycles 1 through 5). (**d**) UDDS test.

The results of this test are shown in Figure 3c. According to the results obtained, the proposed algorithm has achieved a significant improvement in terms of robustness and accuracy when compared to the traditional DKF algorithm. This improvement is the result of applying the proposed technique to the estimation algorithms for both the model parameters and battery SOC, simultaneously. Nonetheless, the error bound for the proposed method was always within ±1%, which is quite acceptable for an EV application. Table 1 presents the MAE of filters for this test.

Interestingly, the proposed algorithm has significantly outperformed the traditional DKF algorithm. In terms of accuracy, the proposed method achieved an MAE of 0.4% with the EDCKF, while the traditional DCKF was many folds more. In terms of convergence speed, the proposed algorithm converged to the true SOC in a few minutes, while it took the DKF algorithm almost 550 min to converge to the true SOC ±1%. This improvement is due to the enhancement in the accuracy of the proposed algorithm by identifying the correct model of the battery. This relates to estimating both the internal parameters of the model and the SOC of the battery. At the same time, the accuracy is achieved through incorporating the correct noise covariance by virtue of the online estimation of the statistics of the dynamics and measurement noise. The proposed method accounts for estimating the correct noise statistics and at the same time monitoring for possible change in these statistics due to change in the battery's operating conditions.

Practically, the EDKF algorithm is very sensitive to model inaccuracy and can easily become inaccurate or even diverge if a little mismatch between the model voltage and the actual/measured voltage occurs. Hence, integrating the noise identification scheme with the parameter and SOC estimation algorithms in the EDCKF case has reduced the MAE substantially from 7.55% down to 0.04%. This promising result can be utilized to enhance the accuracy and robustness of DKF algorithms in other applications.

3.3. Test 3: Cell UDDS Test

In this test, a UDDS cycle is performed using a 3.6 V cell initially charged at 80% SOC. The purpose of this test is to perform further validation of the proposed technique. Figure 4d shows the UDDS test performed on the tested cell, and Table 1 shows the MAE for the filters.

The results of this test are shown in Figure 5. Similar to with the DST, the proposed approach is superior to the traditional one. Comparing the proposed algorithm to the recently proposed method in [24], the MAE has been reduced by 51% using the proposed algorithm under the same experimental conditions. That is, in [24], the MAE was 0.11%, while in the proposed algorithm it is 0.05% when the EDCKF is used. The results obtained add another evidence of the high estimation accuracy the proposed technique can achieve.

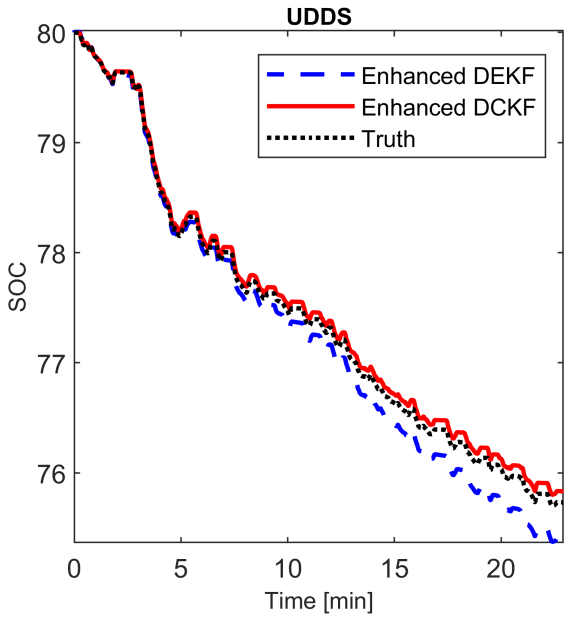

Figure 5. Performance evaluation of the dual Kalman filter variants in the UDDS test.

3.4. Test 4: Cell Constant-Current Discharge Test

To evaluate the impact of temperature variation, a simple discharge test was performed using a 3.6 V Li-ion battery cell at two test temperatures: 0 °C and 20 °C. The cell was fully

charged, allowed to rest for a few minutes, and then discharged using a constant current until its voltage dropped to its cutoff. Before starting the test, the cell was soaked at the test temperature for several hours. The model parameters for the proposed method were originally derived at 20 °C.

For comparison, this test was also used to evaluate the sensitivity of a traditional DKF against the proposed approach. These models were also derived at 20 °C. The sensitivity to temperature variation, $S^{\Delta T}$, is defined as

$$S^{\Delta T} = \frac{MAE_0 - MAE_{20}}{MAE_{20}} \times 100\% \tag{15}$$

where MAE_0 and MAE_{20} are the MAE values at temperatures 0 °C and 20 °C, respectively. A summary of the sensitivity values calculated using (28) are listed in Figure 6.

From Figure 6, it is shown that the traditional DKF is highly sensitive to temperature variation. The reason for this is that the DKF does not account for the statistics of the measurement noise as the proposed method does, which impacts the estimation accuracy when the operating conditions change (in this case, the ambient temperature changed from 20 °C to 0 °C). The proposed method, however, has significantly reduced the sensitivity to temperature variation, which is an important feature when it comes to practical implementation of the proposed algorithm where the ambient temperature is likely to vary on different time scales.

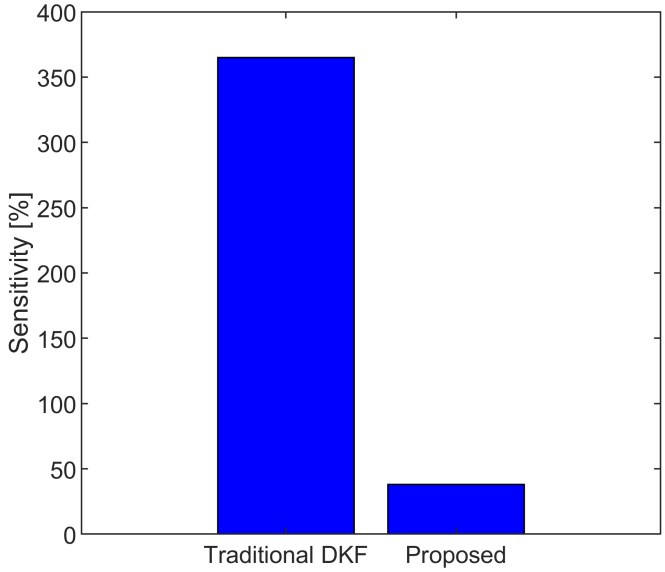

Figure 6. The results of sensitivity to temperature variation.

3.5. Note on the Confidence of KF Estimates

The KF approach provides a measure of the confidence of the estimates it computes. This measure is the state covariance, P, from which one could compute the confidence intervals represented by the 3σ confidence level. In Figure 7, the DKF estimates are provided along with the 3σ confidence bounds in both the SOC estimate and the model parameter estimate. It is noticed that the DCKF results are accompanied by less certain state estimates while the DEKF results show an opposite trend. It is argued that the EKF-based approach suffers from errors arising from linearization, which the CKF estimates generally avoid through the process associated with propagating the predictions using the cubature points better handling nonlinearities in the dynamics and measurements models. As shown in Table 1, however, the DCKF consistently outperforms its counterpart in both the traditional and enhanced testing scenarios, even though its estimates are associated with higher uncertainty.

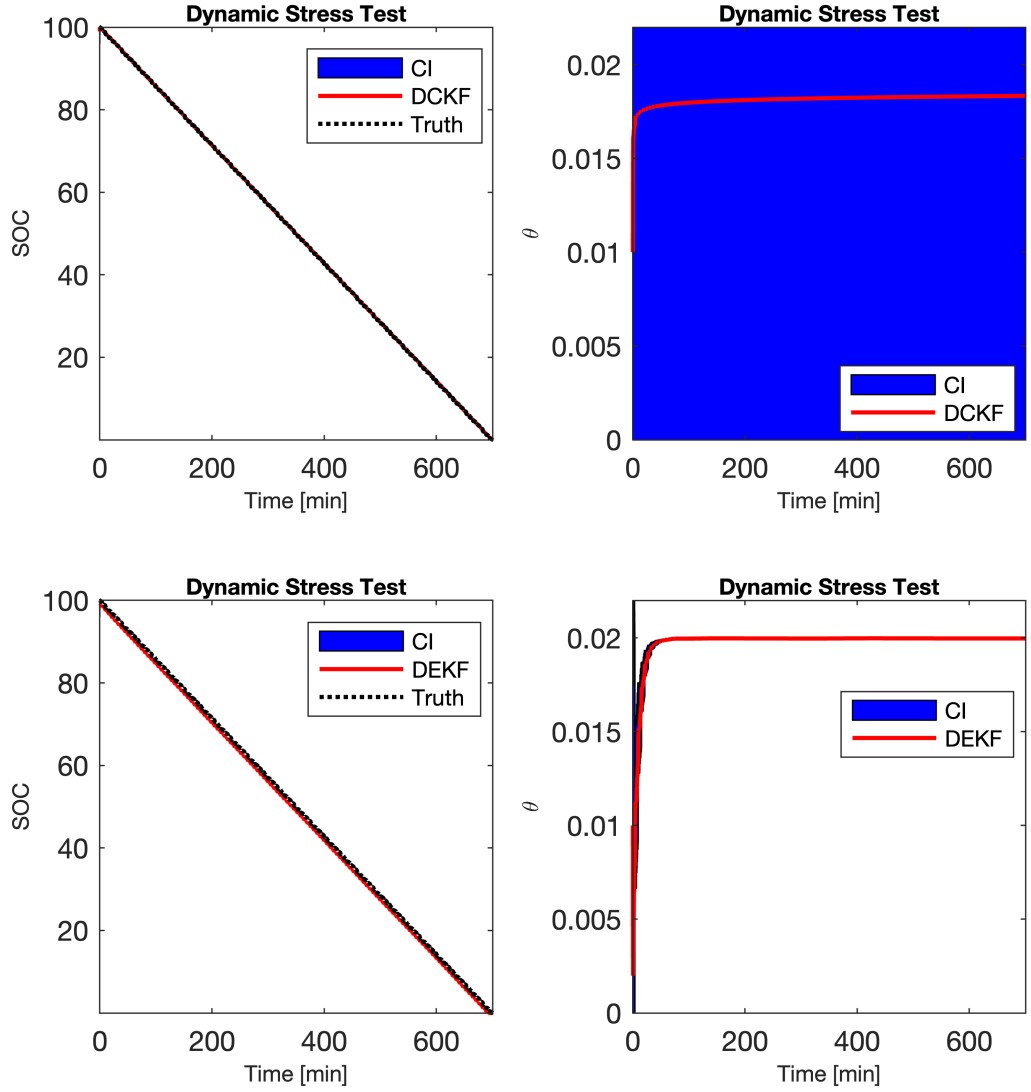

Figure 7. DST test confidence intervals for the DCKF in SOC estimation (**top left**) and internal resistance estimation (**top right**) as well as confidence intervals the DEKF in SOC estimation (**bottom left**) and internal resistance estimation (**bottom right**).

4. Summary and Conclusions

This paper proposed a modified DKF for battery SOC estimation. Among many advantages, the proposed technique has high estimation accuracy, low error bounds, and robust performance. The performance of the proposed technique is validated experimentally using standardized DST and UDDS procedures as well as other less dynamic tests. Results show that the proposed technique has a superior performance over existing algorithms. The technique has also provided accurate and robust results when the temperature was varied from 20 °C to 0 °C, as verified experimentally.

From a practical point of view, improving the stability of the SOC estimation algorithm and enhancing its immunity to temperature variation are vital for improving the overall energy management of the battery. Reducing the error bounds is another key for enhancing the EV's battery performance. Particularly, in battery EVs (BEVs), reducing the error bounds reduces the range anxiety and increases the runtime of the battery. In hybrid EVs (HEVs), reducing the error bounds improves the energy management and hence the fuel-efficiency of the vehicle. By improving the accuracy, stability, and immunity to temperature variation, the battery runtime and service-life can be extended. It shall be noted, however, that the

accuracy of the proposed algorithm, as in other KF-based algorithms, is dictated mainly by the dynamic model used with the algorithm.

With the steady high demand on Li-ion batteries in the EV industry, such battery monitoring techniques are expected to replace traditional techniques for different EV types. Future related research must focus on analyzing the aging of the battery and the temperature impact on the SOC estimation accuracy and robustness.

Author Contributions: Conceptualization, M.A.-H. and A.A.H.; methodology, M.A.-H.; software, A.W.; validation, A.W., M.A.-H. and A.A.H.; formal analysis, A.W.; investigation, M.A.-H.; resources, A.A.H.; data curation, A.A.H. and A.W.; writing—original draft preparation, A.A.H., A.W. and M.A.-H.; writing—review and editing, A.A.H. and M.A.-H.; visualization, A.W.; supervision, M.A.-H.; project administration, M.A.-H. and A.A.H.; funding acquisition, M.A.-H. All authors have read and agreed to the published version of the manuscript.

Funding: This work was supported in part by the American University of Sharjah under the Open Access Program.

Institutional Review Board Statement: Not applicable.

Informed Consent Statement: Not applicable.

Data Availability Statement: Not applicable.

Acknowledgments: This paper represents the opinions of the author(s) and does not mean to represent the position or opinions of the American University of Sharjah.

Conflicts of Interest: The authors declare no conflict of interest.

References

1. Gao, L.; Liu, S.; Dougal, R.A. Dynamic lithium-ion battery model for system simulation. *IEEE Trans. Components Packag. Technol.* **2002**, *25*, 495–505. [CrossRef]
2. Singh, A.; Izadian, A.; Anwar, S. Fault diagnosis of Li-Ion batteries using multiple-model adaptive estimation. In Proceedings of the IECON Proceedings (Industrial Electronics Conference), Vienna, Austria, 10–13 November 2013; pp. 3524–3529. [CrossRef]
3. Chen, M.; Rincón-Mora, G.A. Accurate electrical battery model capable of predicting runtime and I–V performance. *IEEE Trans. Energy Convers.* **2006**, *21*, 504–511. [CrossRef]
4. Abu-Sharkh, S.; Doerffel, D. Rapid test and non-linear model characterisation of solid-state lithium-ion batteries. *J. Power Sources* **2004**, *130*, 266–274. [CrossRef]
5. Hussein, A.A. Experimental modeling and analysis of lithium-ion battery temperature dependence. In Proceedings of the IEEE Applied Power Electronics Conference and Exposition, Charlotte, NC, USA, 5–19 March 2015; pp. 1084–1088. [CrossRef]
6. Hussein, A.A.; Fardoun, A.A.; Stephen, S.S. An Ultrafast Maximum Power Point Tracking Technique for Optimal Battery Charging. *IEEE Trans. Sustain. Energy* **2017**, *8*, 1321–1329. [CrossRef]
7. Hussein, A.A.; Fardoun, A.A.; Stephen, S.S. An online frequency tracking algorithm using terminal voltage spectroscopy for battery optimal charging. *IEEE Trans. Sustain. Energy* **2016**, *7*, 32–40. [CrossRef]
8. He, W.; Pecht, M.; Flynn, D.; Dinmohammadi, F. A Physics-Based Electrochemical Model for Lithium-Ion Battery State-of-Charge Estimation Solved by an Optimised Projection-Based Method and Moving-Window Filtering. *Energies* **2018**, *11*, 2120. [CrossRef]
9. Yang, Z.; Patil, D.; Fahimi, B. Electrothermal Modeling of Lithium-Ion Batteries for Electric Vehicles. *IEEE Trans. Veh. Technol.* **2019**, *68*, 170–179. [CrossRef]
10. Zhou, J.; Xing, B.; Wang, C. A review of lithium ion batteries electrochemical models for electric vehicles. *E3S Web Conf.* **2020**, *185*, 04001. [CrossRef]
11. He, H.; Xiong, R.; Zhang, X.; Sun, F.; Fan, J. State-of-charge estimation of the lithium-ion battery using an adaptive extended Kalman filter based on an improved Thevenin model. *IEEE Trans. Veh. Technol.* **2011**, *60*, 1461–1469. [CrossRef]
12. Plett, G.L. Extended Kalman filtering for battery management systems of LiPB-based HEV battery packs—Part 3. State and parameter estimation. *J. Power Sources* **2004**, *134*, 277–292. [CrossRef]
13. Zhang, F.; Liu, G.; Fang, L. A battery state of charge estimation method with extended Kalman filter. In Proceedings of the IEEE/ASME International Conference on Advanced Intelligent Mechatronics, Xi'an, China, 2–5 July 2008; pp. 1008–1013. [CrossRef]
14. Qiu, S.; Chen, Z.; Masrur, M.A.; Murphey, Y.L. Battery hysteresis modeling for state of charge estimation based on Extended Kalman Filter. In Proceedings of the 2011 6th IEEE Conference on Industrial Electronics and Applications, Beijing, China, 21–23 June 2011; pp. 184–189. [CrossRef]

15. Di Domenico, D.; Fiengo, G.; Stefanopoulou, A. Lithium-ion Battery state of charge estimation with a Kalman filter based on a electrochemical model. In Proceedings of the IEEE International Conference on Control Applications, San Antonio, TX, USA, 3–5 September 2008; pp. 702–707. [CrossRef]
16. Yan, W.; Tian-Ming, Y.; Bao-Jie, L. Lead-acid power battery management system basing on Kalman filtering. In Proceedings of the 2008 IEEE Vehicle Power and Propulsion Conference, Harbin, China, 3–5 September 2008. [CrossRef]
17. Windarko, N.A.; Choi, J.; Chung, G.B. SOC estimation of LiPB batteries using Extended Kalman Filter based on high accuracy electrical model. In Proceedings of the 8th International Conference on Power Electronics—ECCE Asia: "Green World with Power Electronics", ICPE 2011-ECCE Asia, Jeju, Korea, 30 May–3 June 2011; pp. 2015–2022. [CrossRef]
18. Wadi, A.; Abdel-Hafez, M.; Hussein, A.A.; Khawaja, F. Alleviating Dynamic Model Uncertainty Effects for Improved Battery SOC Estimation of EVs in Highly Dynamic Environments. *IEEE Trans. Veh. Technol.* **2021**, *70*, 6554–6566. [CrossRef]
19. Partovibakhsh, M.; Liu, G. An adaptive unscented kalman filtering approach for online estimation of model parameters and state-of-charge of lithium-ion batteries for autonomous mobile robots. *IEEE Trans. Control. Syst. Technol.* **2015**, *23*, 357–363. [CrossRef]
20. He, H.; Xiong, R.; Guo, H. Online estimation of model parameters and state-of-charge of LiFePO4 batteries in electric vehicles. *Appl. Energy* **2012**, *89*, 413–420. [CrossRef]
21. Wan, E.A.; Van Der Merwe, R. The unscented Kalman filter for nonlinear estimation. In Proceedings of the IEEE 2000 Adaptive Systems for Signal Processing, Communications, and Control Symposium, Lake Louise, AB, Canada, 4 October 2000; pp. 153–158. [CrossRef]
22. Shehab El Din, M.; Abdel-Hafez, M.F.; Hussein, A.A. Enhancement in Li-Ion battery cell state-of-charge estimation under uncertain model statistics. *IEEE Trans. Veh. Technol.* **2016**, *65*, 4608–4618. [CrossRef]
23. Shehab El Din, M.; Hussein, A.A.; Abdel-Hafez, M.F. Improved battery SOC estimation accuracy using a modified UKF with an adaptive cell model under real EV operating conditions. *IEEE Trans. Transp. Electrif.* **2018**, *4*, 408–417. [CrossRef]
24. Wadi, A.; Abdel-Hafez, M.F.; Hussein, A.A. Mitigating the Effect of Noise Uncertainty on the Online State-of-Charge Estimation of Li-Ion Battery Cells. *IEEE Trans. Veh. Technol.* **2019**, *68*, 8593–8600. [CrossRef]
25. Hussein, A.A. Kalman Filters versus Neural Networks in Battery State-of-Charge Estimation: A Comparative Study. *Int. J. Mod. Nonlinear Theory Appl.* **2014**, *3*, 199–209. [CrossRef]
26. Chaoui, H.; Ibe-Ekeocha, C.C. State of Charge and State of Health Estimation for Lithium Batteries Using Recurrent Neural Networks. *IEEE Trans. Veh. Technol.* **2017**, *66*, 8773–8783. [CrossRef]
27. Lipu, M.S.; Hannan, M.A.; Hussain, A.; Saad, M.H.; Ayob, A.; Blaabjerg, F. State of Charge Estimation for Lithium-Ion Battery Using Recurrent NARX Neural Network Model Based Lighting Search Algorithm. *IEEE Access* **2018**, *6*, 28150–28161. [CrossRef]
28. Hannan, M.A.; Lipu, M.S.; Hussain, A.; Saad, M.H.; Ayob, A. Neural network approach for estimating state of charge of lithium-ion battery using backtracking search algorithm. *IEEE Access* **2018**, *6*, 10069–10079. [CrossRef]
29. Hossain Lipu, M.S.; Hussain, A.; Saad, M.H.; Ayob, A.; Hannan, M.A. Improved recurrent NARX neural network model for state of charge estimation of lithium-ion battery using pso algorithm. In Proceedings of the ISCAIE 2018—2018 IEEE Symposium on Computer Applications and Industrial Electronics, Penang, Malaysia, 28–29 April 2018; pp. 354–359. [CrossRef]
30. Yu, Z.; Xiao, L.; Li, H.; Zhu, X.; Huai, R. Model Parameter Identification for Lithium Batteries Using the Coevolutionary Particle Swarm Optimization Method. *IEEE Trans. Ind. Electron.* **2017**, *64*, 5690–5700. [CrossRef]
31. Hossain Lipu, M.S.; Hannan, M.A.; Hussain, A.; Saad, M.H.; Ayob, A.; Uddin, M.N. Extreme learning machine model for state-of-charge estimation of lithium-ion battery using gravitational search algorithm. *IEEE Trans. Ind. Appl.* **2019**, *55*, 4225–4234. [CrossRef]
32. Chemali, E.; Kollmeyer, P.J.; Preindl, M.; Emadi, A. State-of-charge estimation of Li-ion batteries using deep neural networks: A machine learning approach. *J. Power Sources* **2018**, *400*, 242–255. [CrossRef]
33. Wadi, A.; Abdel-Hafez, M.F.; Hussein, A.A. Enhanced EKF Method for State-of-Charge Estimation of Electric Vehicles' Li-ion Batteries under Highly Dynamic Power Profiles. In Proceedings of the 2021 4th International Symposium on Advanced Electrical and Communication Technologies (ISAECT), Alkhobar, Saudi Arabia, 6–8 December 2021; pp. 1–6. [CrossRef]
34. Rubagotti, M.; Onori, S.; Rizzoni, G. Automotive Battery Prognostics Using Dual Extended Kalman Filter. In Proceedings of the ASME 2009 Dynamic Systems and Control Conference, Hollywood, CA, USA, 12–14 October 2009. [CrossRef]
35. Li, S.; Pischinger, S.; He, C.; Liang, L.; Stapelbroek, M. A comparative study of model-based capacity estimation algorithms in dual estimation frameworks for lithium-ion batteries under an accelerated aging test. *Appl. Energy* **2018**, *212*, 1522–1536. [CrossRef]
36. Wu, J.; Jiao, C.; Chen, M.; Chen, J.; Zhang, Z. SOC Estimation of Li-ion Battery by Adaptive Dual Kalman Filter under Typical Working Conditions. In Proceedings of the 2019 IEEE 3rd International Electrical and Energy Conference (CIEEC), Beijing, China, 7–9 September 2019; pp. 1561–1567. [CrossRef]
37. Wassiliadis, N.; Adermann, J.; Frericks, A.; Pak, M.; Reiter, C.; Lohmann, B.; Lienkamp, M. Revisiting the dual extended Kalman filter for battery state-of-charge and state-of-health estimation: A use-case life cycle analysis. *J. Energy Storage* **2018**, *19*, 73–87. [CrossRef]
38. Zhao, S.; Duncan, S.R.; Howey, D.A. Observability Analysis and State Estimation of Lithium-Ion Batteries in the Presence of Sensor Biases. *IEEE Trans. Control. Syst. Technol.* **2017**, *25*, 326–333. [CrossRef]
39. Haykin, S. *Kalman Filtering and Neural Networks*; Wiley: New York, NY, USA, 2002.

40. Collins, J.P.; Langley, R.B. *Possible Weighting Schemes for GPS Carrier Phase Observations in the Presence of Multipath*; Technical Report; Geodetic Research Laboratory: Fredericton, NB, Canada, 1999.
41. Mohamed, A.H.; Schwarz, K.P. Adaptive Kalman filtering for INS/GPS. *J. Geod.* **1999**, *73*, 193–203. [CrossRef]
42. Xia, B.; Wang, H.; Tian, Y.; Wang, M.; Sun, W.; Xu, Z. State of Charge Estimation of Lithium-Ion Batteries Using an Adaptive Cubature Kalman Filter. *Energies* **2015**, *8*, 5916–5936. [CrossRef]